

Extended Scalar Sector and Fat Jets

M. Rauch ^a

Institute for Theoretical Physics, Karlsruhe Institute of Technology, Karlsruhe, Germany

After a discovery of the Higgs boson the next question is what are its couplings. At the LHC there should be many observable channels which can be exploited to measure the relevant parameters in the Higgs sector. Using the SFitter framework we map these measurements onto the parameter space of a weak-scale effective theory with free Higgs boson couplings. Our analysis benefits from the parameter determination tools and the error treatment used in new-physics searches, to study individual parameters and their error bars as well as parameter correlations. A special focus we will put on recent analyses using jet substructure techniques.

1 Introduction

Understanding electro-weak symmetry breaking is one of the main goals of the LHC. In the Standard Model (SM) this is done spontaneously, and achieved by an $SU(2)$ doublet, the Higgs field ^{1,2}, which obtains a vacuum expectation value (vev). Three degrees of freedom become the longitudinal modes of W and Z bosons, while one remains as a physical scalar, the Higgs boson. The gauge boson masses arise from the kinetic term of the Higgs field in the Lagrangian $(D_\mu\Phi)^\dagger(D^\mu\Phi)$, which leads to $WWHH$ and $ZZHH$ terms, and replacing the Higgs field by its vev then to the masses. As these and the electromagnetic coupling are measured, this allows to determine the vev $v = 246$ GeV before actually observing the Higgs boson. Fermion masses we obtain from terms $y_f H\bar{\Psi}\Psi$. The Yukawa couplings y_f are a priori free parameters in the Lagrangian, but can be traded for the known fermion masses $m_f = y_f \cdot v$. This also means that the coupling of the Higgs to fermions scales as the fermion masses.

The mass of the Higgs boson is the only unknown parameter in the SM. Electroweak precision tests tell us that it should be relatively light, just above the limit of 114.4 GeV from direct searches at LEP ^{3,4}. Therefore we can use the theoretically predicted coupling values and test this ^{5,6} against future LHC measurements ^{7,8}. Thereby we assume that the discrete quantum numbers, like spin and CP structure, of the boson are known ⁹ and identical to the SM. Still there are many possible models which can generate such deviations. Examples include simple extensions like adding another Higgs doublet, which is e.g. required in supersymmetry ^{10,11}, or composite models ¹², where the Higgs emerges as a pseudo-Goldstone boson from a strongly-interacting sector.

A correct treatment of errors is a crucial part for LHC parameter studies. Statistical errors from event counting are of the Poisson type. Systematic errors are correlated between individual measurements, so we need to include the full correlation matrix. Theory errors are best described as box-shaped using the RFit scheme ¹³. Using the SFitter tool ¹⁴ we can construct a fully-dimensional log-likelihood map of the parameter space. If we want to ask more specific questions,

^afor the SFitter collaboration

Table 1: Signatures included in our analysis for a Higgs mass of 120 GeV. The Standard Model event numbers for 30 fb^{-1} include cuts^{16,6}. The factor after the background rates describes how many events are used to extrapolate into the signal region. The last two columns give the one-sigma experimental and theory error bars on the signal. Table taken from Ref.⁶

production	decay	$S + B$	B	S	$\Delta S^{(\text{exp})}$	$\Delta S^{(\text{theo})}$
$gg \rightarrow H$	ZZ	13.4	6.6 ($\times 5$)	6.8	3.9	0.8
qqH	ZZ	1.0	0.2 ($\times 5$)	0.8	1.0	0.1
$gg \rightarrow H$	WW	1019.5	882.8 ($\times 1$)	136.7	63.4	18.2
qqH	WW	59.4	37.5 ($\times 1$)	21.9	10.2	1.7
$t\bar{t}H$	$WW(3\ell)$	23.9	21.2 ($\times 1$)	2.7	6.8	0.4
$t\bar{t}H$	$WW(2\ell)$	24.0	19.6 ($\times 1$)	4.4	6.7	0.6
inclusive	$\gamma\gamma$	12205.0	11820.0 ($\times 10$)	385.0	164.9	44.5
qqH	$\gamma\gamma$	38.7	26.7 ($\times 10$)	12.0	6.5	0.9
$t\bar{t}H$	$\gamma\gamma$	2.1	0.4 ($\times 10$)	1.7	1.5	0.2
WH	$\gamma\gamma$	2.4	0.4 ($\times 10$)	2.0	1.6	0.1
ZH	$\gamma\gamma$	1.1	0.7 ($\times 10$)	0.4	1.1	0.1
qqH	$\tau\tau(2\ell)$	26.3	10.2 ($\times 2$)	16.1	5.8	1.2
qqH	$\tau\tau(1\ell)$	29.6	11.6 ($\times 2$)	18.0	6.6	1.3
$t\bar{t}H$	$b\bar{b}$	244.5	219.0 ($\times 1$)	25.5	31.2	3.6
WH/ZH	$b\bar{b}$	228.6	180.0 ($\times 1$)	48.6	20.7	4.0

this must be reduced to lower-dimensional ones. Bayesian marginalization and Frequentist profile likelihoods are the two techniques we use, where the choice depends on the specific question we want to ask.

In this article we will first review the LHC measurement channels which enter into our analysis. A particular emphasis we will put on the recently developed method of using jet substructure techniques¹⁵. Then we will present and discuss our results for Standard Model data. We focus on a Higgs boson of $m_H = 120 \text{ GeV}$, which is the preferred region from electro-weak precision data.

2 Measurements

At the LHC there are four main production modes of the Higgs boson: gluon fusion, weak-boson-fusion, associated production with vector bosons and associated production with a top-quark pair¹⁷. They need to be combined with the corresponding decay channels. For a light Higgs boson, like one with 120 GeV as we consider here, the main decay mode is into a pair of bottom quarks. Also decays via off-shell W and Z pairs lead to observable channels. Decays into taus can only be combined with weak-boson fusion¹⁸, as we need to reconstruct the invariant mass of the tau pair, which is only known in the collinear limit¹⁹. This channel is one of the discovery modes for a light Higgs and also allows us to determine its mass with a precision of $\sim 5 \text{ GeV}$. The decay into photons is loop-induced and therefore only has a small branching fraction of $\sim 0.26\%$ for a 120 GeV Higgs. Nevertheless the flat background, which is well subtractable by a side-band analysis, and a good $\gamma\gamma$ mass resolution make this mode a discovery channel and allow us to measure the mass with a precision $\mathcal{O}(100 \text{ MeV})$.

In total we obtain the channels described in Table 1. The numerical values for Higgs production we get from Ref.²⁰ and for the decay from a modified version of HDECAY²¹. We do not include any channel which will only be measured at a later stage like the second-generation fermions. Such channels typically determine one additional parameter and therefore do not feed

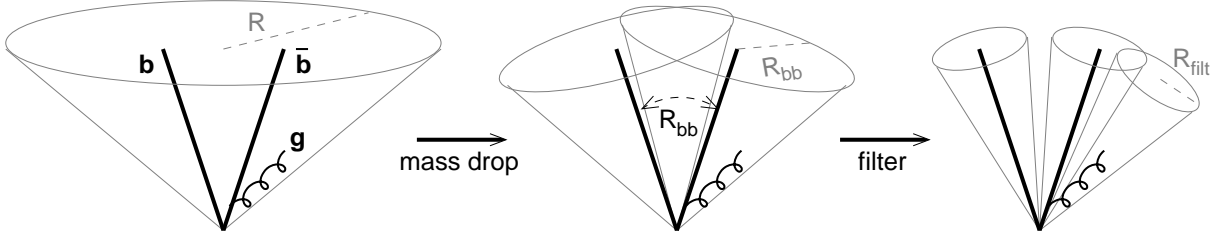


Figure 1: Illustration of the subjet algorithm. Starting with a fat jet, we first undo the last stages of the jet clustering until we have identified the bottom jets. We then apply a filter to remove the underlying event while retaining hard radiation from the Higgs decay products. Figure taken from Ref. ¹⁵.

back into the analysis here. This also includes the Higgs self-couplings, which are important to establish the nature of electro-weak symmetry breaking, but are notoriously hard to determine experimentally ^{22,23}.

3 Subjet Techniques

In this section we will discuss in more detail the recent development of jet substructure techniques. Its presentation is based on the original paper ¹⁵. We consider associated production with vector-bosons with Higgs decays into a bottom-quark pair. A standard analysis would be overwhelmed by the large QCD background. Therefore we only consider a regime where both bosons are back-to-back and have large transverse momenta. For transverse momenta of the Higgs larger than 200 GeV only about one in twenty events survives. This is compensated by several advantages. The boost leads to central decay products, which can be tagged more easily. Also on-shell top quarks cannot simulate this kind of behavior and are no longer a background. Finally, the channel with Z decaying into neutrinos becomes visible as large missing transverse energy.

Such a boost also means that often the jet reconstruction algorithm will not be able to resolve both bottom quarks. Instead it will combine them into a single fat jet. For $R \simeq \frac{3m_H}{p_T}$ this happens in roughly 75% of the cases. Therefore we need to identify such a fat jet. The Cambridge/Aachen jet algorithm ²⁴ has thereby shown to give the best results for the following procedure. Starting with a high- p_T jet j we first undo the last stage of clustering so that we obtain two subjets j_1, j_2 with $m_{j_1} > m_{j_2}$. Next we check if there has been a significant mass drop $\max(m_{j_1}, m_{j_2}) < 0.67m$. Additionally we test if the splitting is not too asymmetric $y = \frac{\min(p_{T,j_1}^2, p_{T,j_2}^2)}{m_j^2} \Delta R_{j_1, j_2}^2 > 0.09$. If either of the conditions is not fulfilled, we take j_1 as j and repeat the steps.

Otherwise we check if both subjets have b tags and if not, reject the event. This candidate Higgs event is then filtered. We resolve the structure with a finer R separation $R_{\text{filt}} = \min(0.3, R_{bb}/2)$ and take the three hardest subjets. These are typically the two b jets and the leading radiation. A graphical description of the algorithm is depicted in Fig. 1.

The ATLAS collaboration has performed a full study using these techniques ²⁵ and they obtain a statistical significance of 3.7σ for a 120 GeV Higgs boson and a luminosity of 30 fb^{-1} . Including 15% systematic uncertainty a significance of 3.0σ can be achieved.

This method has also been applied to associated Higgs production with top quarks and bottom quark decays ²⁶. Here the subjet technique can help reduce the combinatorial background, which degrades the standard analysis. For a luminosity of 100 fb^{-1} the statistical significance of this channel is 4.1 standard deviations. Additionally it has been shown that further combining different subjet techniques can enhance the statistical significance even more ²⁷.

4 Computational Setup

For our analysis we assume a generalization of the SM Higgs sector with arbitrary couplings. Any coupling to particle j present in the SM we modify according to

$$g_{jjH} \rightarrow g_{jjH}^{\text{SM}}(1 + \Delta_{jjH}) \quad (1)$$

where the Δ_{jjH} are independent of each other. As a global sign change in the Higgs couplings is not observable, we can take g_{WWH} to be always positive, or $\Delta_{WWH} > -1$. Additionally loop-induced couplings to the photon and gluon are relevant. Here also the modified tree-level couplings enter. Also we allow for further dimension-five operators from new physics in the Lagrangian. An example for such a term are the additional loop contributions from supersymmetric partners. Therefore these couplings are modified to

$$g_{jjH} \rightarrow g_{jjH}^{\text{SM}}(1 + \Delta_{jjH}^{\text{SM}} + \Delta_{jjH}) , \quad (2)$$

where g_{jjH}^{SM} is the loop-induced coupling in the SM, Δ_{jjH}^{SM} the contribution from modified tree-level couplings and Δ_{jjH} the additional dimension-five part. We also include the masses of the Higgs boson and the top- and bottom-quark into our parameter set. The errors on their measurements are large enough that their influence on the coupling determination should be taken into account.

Furthermore we need to specify our treatment of the total width. This could also receive further contributions

$$\Gamma_{\text{tot}} = \Gamma_{\text{tot}}^{\text{SM}}(1 + \Delta_{\Gamma}) , \quad \Delta_{\Gamma} \geq 0 . \quad (3)$$

A simultaneous scaling of all couplings and the total width where $g^4/\Gamma_{\text{tot}} = \text{const.}$ leaves all rates the same and we therefore cannot distinguish this. We will hence fix the total width to the sum of observed partial widths.

The treatment of errors is a crucial part of the analysis. Statistical errors on individual channels are from counting experiments and therefore of Poisson type. The systematic errors are taken as fully correlated between the channels. They are derived from large event samples and can therefore safely assumed to be Gaussian. To combine these two types of errors we have devised an approximate formula of summing the inverse of the log-likelihoods⁶

$$\frac{1}{\tilde{\chi}^2} \equiv \frac{1}{-2 \log L} = \sum_i \frac{1}{-2 \log L_i} . \quad (4)$$

For a sum of Gaussians this gives the correct result of adding the errors in quadrature, while we have checked numerically that in all other cases we have a very good agreement with the exact way of a mathematical convolution. For theory errors we use the RFit prescription¹³. For a deviation smaller than the theory error, the partial log-likelihood of the measurement is zero, while outside of this region it falls off with the combined experimental error. For the assumed numerical values of the errors we refer to Ref.⁶.

5 Results

5.1 Likelihood map

In Fig. 2 we show distributions for the three couplings Δ_{WWH} , Δ_{ttH} and Δ_{bbH} . In the left top row we show profile likelihoods for an unsmeared data set with an integrated luminosity of 30 fb^{-1} . Additional contributions to the loop-induced couplings we set to zero here. For all couplings we see a peak at the correct solution of $\Delta = 0$. For both ttH and bbH a second peak at $\Delta = -2$ appears, which corresponds to a flipped sign of the coupling. For the top-quark the

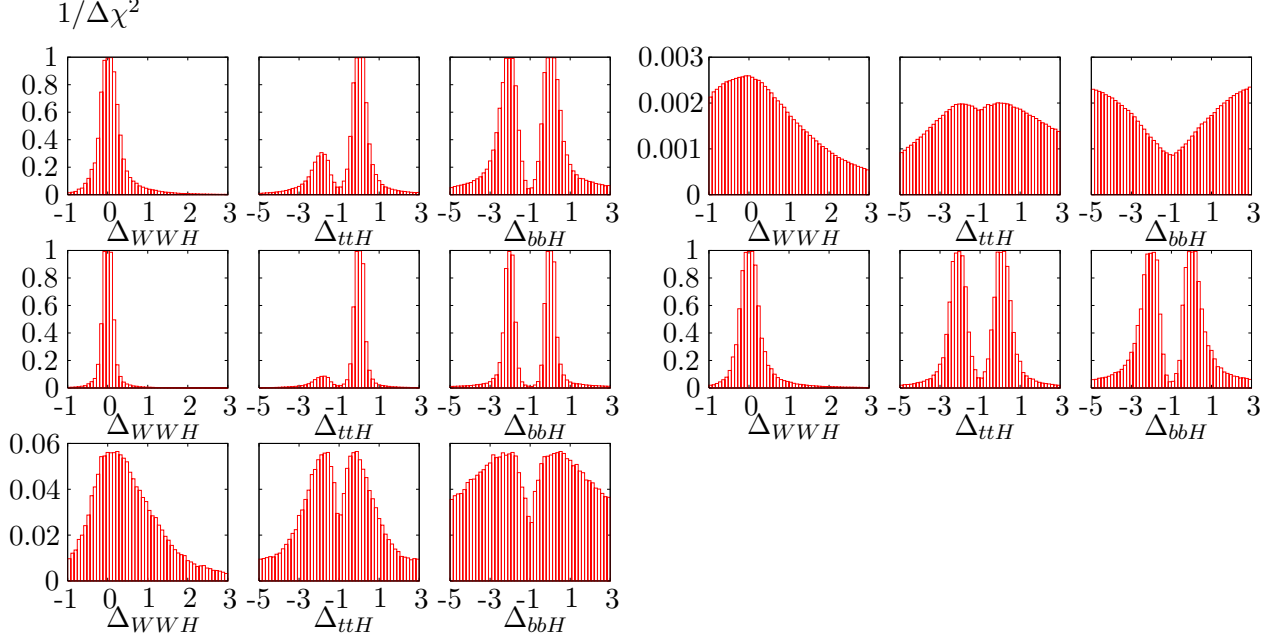


Figure 2: Distributions for different couplings. Starting from the top left set with profile likelihoods for an unsmeared data set with an integrated luminosity of 30 fb^{-1} and no effective couplings, we modify these in the other sets: Bayesian marginalization (top right), 300 fb^{-1} (middle left), including effective coupling (middle right), and smeared data set with effective couplings (bottom). Plots taken from Ref. ⁶.

likelihood of this solution is strongly reduced. The interference with a W -loop in the effective Higgs-photon coupling allows us to determine the correct sign. In principle the same effect would also be true for the bottom quark. Its contribution to the effective photon or gluon coupling, which would fix the sign with respect to ttH , is too small to see an effect.

On the right-hand side we take the same input in the top row, but now use Bayesian marginalization. The interference effect, which breaks the sign degeneracy in ttH , is completely washed out by volume effects. The bbH coupling shows a peculiar effect. Large values of the coupling are more likely than the correct one. The branching ratio into bottom quarks is much less affected by changing the coupling than other ones, because this also increases the total width significantly and the effect partly cancels. On the other hand large values allow larger changes in the other couplings without relevant changes of the overall rates. Therefore we have more parameter space available, so this is a pure volume effect. To understand the correlations we see Bayesian probabilities are less useful here and therefore we will show only profile likelihoods from now on.

On the left-hand side of the middle row of Figure 2 we show a ten-fold increase of luminosity to 300 fb^{-1} compared to the top row. The general features stay unchanged, while the errors go down significantly, because the precision is primarily statistically limited. On the right-hand side we allow for additional contributions to the ggH and $\gamma\gamma H$ couplings at 30 fb^{-1} . We see that both peaks for the top-quark coupling now have the same height. The effective photon coupling can no longer break the sign degeneracy of ttH . Any mismatch is compensated by appropriately dialing the new term.

In the bottom row we move from the true data set to a smeared one. This we have obtained by randomly smearing each measurement according to its errors. We see that the overall behavior does not change significantly. The best-fitting points move slightly away from their true values. Also the peak structure gets broader, as different measurements try to pull the parameters into different directions.

Table 2: Errors on the measurements form 10000 toy experiments. We quote absolute errors on the couplings for 30 fb^{-1} , where additional contributions to the ggH and $\gamma\gamma H$ couplings are either forbidden or allowed. For the latter we also show errors on the ratio of the coupling to WWH . Table taken from Ref. ⁶.

	no eff. couplings			with eff. couplings			ratio $\Delta_{jjH/WWH}$		
	σ_{symm}	σ_{neg}	σ_{pos}	σ_{symm}	σ_{neg}	σ_{pos}	σ_{symm}	σ_{neg}	σ_{pos}
Δ_{WWH}	± 0.23	-0.21	$+0.26$	± 0.24	-0.21	$+0.27$	—	—	—
Δ_{ZZH}	± 0.36	-0.40	$+0.35$	± 0.31	-0.35	$+0.29$	± 0.41	-0.40	$+0.41$
Δ_{ttH}	± 0.41	-0.37	$+0.45$	± 0.53	-0.65	$+0.43$	± 0.51	-0.54	$+0.48$
Δ_{bbH}	± 0.45	-0.33	$+0.56$	± 0.44	-0.30	$+0.59$	± 0.31	-0.24	$+0.38$
$\Delta_{\tau\tau H}$	± 0.33	-0.21	$+0.46$	± 0.31	-0.19	$+0.46$	± 0.28	-0.16	$+0.40$
$\Delta_{\gamma\gamma H}$	—	—	—	± 0.31	-0.30	$+0.33$	± 0.30	-0.27	$+0.33$
Δ_{ggH}	—	—	—	± 0.61	-0.59	$+0.62$	± 0.61	-0.71	$+0.46$
m_H	± 0.26	-0.26	$+0.26$	± 0.25	-0.26	$+0.25$	—	—	—
m_b	± 0.071	-0.071	$+0.071$	± 0.071	-0.071	$+0.072$	—	—	—
m_t	± 1.00	-1.03	$+0.98$	± 0.99	-1.00	$+0.98$	—	—	—

5.2 Error determination

To determine the errors we perform 10000 toy experiments, where we have smeared each measurement around the true data point including all experimental and theory errors. The resulting distribution we then fit with a Gaussian and extract σ_{symm} . As the errors are not necessarily symmetric, we also fit two-half Gaussians with the same maximum and same height at the maximum, but different errors below (σ_{neg}) and above (σ_{pos}) the maximum. The fit-region is in all cases the central part within one standard deviation.

From the results in Table 2 we see that the mass measurements hardly play any role. Their distributions are completely symmetric Gaussians and the errors correspond to the input values. The WWH coupling is the most precisely determined one. Its value does not change once we allow effective couplings, which means that the indirect determination via the loop-induced $g_{\gamma\gamma H}$ is not important for a precise determination. The situation is completely different for ttH . As main contribution to g_{ggH} and sub-leading to $g_{\gamma\gamma H}$ the effective couplings significantly increase the error. Both main measurements for $\tau\tau H$ and bbH are linked with a production mode where the WWH coupling enters, namely vector-boson fusion and associated production with subjet techniques, respectively. Therefore effective couplings do not change the errors here. The error on ZZH shows a particular effect. It decreases once we include effective couplings. This is an effect of the correlations between measurements. The main determination channel is gluon-fusion production with Higgs decay into a pair of Z bosons. Without effective couplings the production side is linked to the top-quark coupling, which is constrained by many other channels. Including them, this connection is removed and the error on the measurement need not be compensated by changing ZZH alone. Instead both can be changed, and due to the positive correlation between the two couplings this reduces the error.

One might expect that forming ratios of coupling constants could improve the precision, as always certain combinations appear in our rate measurements. Due to its relatively small error the WWH coupling serves well as base value. Hence we also define a deviation on the coupling ratio to the WWH coupling as

$$\frac{g_{jjH}}{g_{WWH}} \rightarrow \left(\frac{g_{jjH}}{g_{WWH}} \right)^{\text{SM}} \left(1 + \Delta_{jjH/WWH} \right). \quad (5)$$

The results we show in the right column of Table 2. In particular bbH benefits from forming the ratio. This is due to the total width, which appears in all measurements. The bbH coupling

yields the largest contribution for a light Higgs boson and this leads to strong correlations to all other couplings.

6 Conclusions

In this article we have studied the determination of Higgs couplings at the LHC. As model we have assumed the Standard Model with free Higgs couplings, so that we are independent from the exact realization of new physics, if any. Using SFitter as a tool we map a set of LHC measurements onto the multi-dimensional parameter space. We have taken effects from statistical, correlated systematic and box-shaped theory errors into account.

We find that we can determine the couplings with a precision of 20 – 40%. The improved accuracy from the newly developed subset techniques is thereby an important ingredient. It helps to determine the bottom-quark Higgs coupling, which influences all others via its contribution to the total width.

Acknowledgments

We would like to thank the organizers of “Rencontres de Moriond EW 2010” for the inspiring atmosphere during the workshop and for financial support. We acknowledge support by the Deutsche Forschungsgemeinschaft via the Sonderforschungsbereich/Transregio SFB/TR-9 Computational Particle Physics and the Initiative and Networking Fund of the Helmholtz Association, contract HA-101 (Physics at the Terascale).

References

1. P. W. Higgs, Phys. Lett. **12**, 132 (1964); P. W. Higgs, Phys. Rev. Lett. **13**, 508 (1964); F. Englert and R. Brout, Phys. Rev. Lett. **13**, 321 (1964).
2. A. Djouadi, Phys. Rept. **457**, 1 (2008) V. Büscher and K. Jakobs, Int. J. Mod. Phys. A **20**, 2523 (2005); D. Rainwater, arXiv:hep-ph/0702124.
3. J. Alcaraz *et al.* [LEP Collaborations and ALEPH Collaboration and DELPHI Collaboration an], arXiv:0712.0929 [hep-ex].
4. [ALEPH Collaboration and CDF Collaboration and D0 Collaboration and an], arXiv:0811.4682 [hep-ex].
5. M. Dürrssen, S. Heinemeyer, H. Logan, D. Rainwater, G. Weiglein and D. Zeppenfeld, Phys. Rev. D **70**, 113009 (2004).
6. R. Lafaye, T. Plehn, M. Rauch, D. Zerwas and M. Duhrssen, JHEP **0908**, 009 (2009) [arXiv:0904.3866 [hep-ph]].
7. G. Aad *et al.* [The ATLAS Collaboration], arXiv:0901.0512 [hep-ex].
8. G. L. Bayatian *et al.* [CMS Collaboration], J. Phys. G **34**, 995 (2007).
9. J. R. Dell’Aquila and C. A. Nelson, Phys. Rev. D **33**, 93 (1986).; T. Plehn, D. Rainwater and D. Zeppenfeld, Phys. Rev. Lett. **88**, 051801 (2002); C. P. Buszello, I. Fleck, P. Marquard and J. J. van der Bij, Eur. Phys. J. C **32**, 209 (2004); V. Hankele, G. Klamke, D. Zeppenfeld and T. Figy, Phys. Rev. D **74**, 095001 (2006); C. Ruwiedel, N. Wermes and M. Schumacher, Eur. Phys. J. C **51**, 385 (2007).
10. for a pedagogical introduction see e.g. S. P. Martin, arXiv:hep-ph/9709356; I. J. R. Aitchison, arXiv:hep-ph/0505105; J. F. Gunion and H. E. Haber, Phys. Rev. D **67**, 075019 (2003).
11. H. E. Haber, R. Hempfling and A. H. Hoang, Z. Phys. C **75**, 539 (1997); G. Degrassi, S. Heinemeyer, W. Hollik, P. Slavich and G. Weiglein, Eur. Phys. J. C **28**, 133 (2003);

- T. Hahn, S. Heinemeyer, W. Hollik, H. Rzehak, G. Weiglein and K. Williams, *Pramana* **69**, 861 (2007).
12. J. R. Espinosa, C. Grojean and M. Muhlleitner, arXiv:1003.3251 [hep-ph].
 13. A. Höcker, H. Lacker, S. Laplace and F. Le Diberder, *Eur. Phys. J. C* **21**, 225 (2001); J. Charles, A. Höcker, H. Lacker, F. R. Le Diberder and S. T'Jampens, arXiv:hep-ph/0607246.
 14. R. Lafaye, T. Plehn, M. Rauch and D. Zerwas, *Eur. Phys. J. C* **54**, 617 (2008); for earlier versions of SFitter see: R. Lafaye, T. Plehn and D. Zerwas, arXiv:hep-ph/0404282 and arXiv:hep-ph/0512028.
 15. J. M. Butterworth, A. R. Davison, M. Rubin and G. P. Salam, *Phys. Rev. Lett.* **100**, 242001 (2008).
 16. M. Dührssen, ATL-PHYS-2003-030.
 17. for an overview see e.g. A. Djouadi, *Phys. Rept.* **457**, 1 (2008) [arXiv:hep-ph/0503172].
 18. D. Rainwater, D. Zeppenfeld and K. Hagiwara, *Phys. Rev. D* **59**, 014037 (1999); T. Plehn, D. L. Rainwater and D. Zeppenfeld, *Phys. Rev. D* **61**, 093005 (2000).
 19. R. K. Ellis, I. Hinchliffe, M. Soldate and J. J. van der Bij, *Nucl. Phys. B* **297**, 221 (1988).
 20. M. Spira, arXiv:hep-ph/9510347.
 21. A. Djouadi, J. Kalinowski and M. Spira, *Comput. Phys. Commun.* **108**, 56 (1998).
 22. U. Baur, T. Plehn and D. L. Rainwater, *Phys. Rev. Lett.* **89**, 151801 (2002) and *Phys. Rev. D* **67**, 033003 (2003); A. Dahloff, arXiv:hep-ex/0505022; for a different point of view see also F. Gianotti *et al.*, arXiv:hep-ph/0204087.
 23. T. Plehn and M. Rauch, *Phys. Rev. D* **72**, 053008 (2005); T. Binoth, S. Karg, N. Kauer and R. Rückl, *Phys. Rev. D* **74**, 113008 (2006).
 24. Y. L. Dokshitzer, G. D. Leder, S. Moretti and B. R. Webber, *JHEP* **9708**, 001 (1997) [arXiv:hep-ph/9707323]; M. Wobisch and T. Wengler, arXiv:hep-ph/9907280.
 25. ATLAS Collaboration, ATL-PHYS-PUB-2009-088
 26. T. Plehn, G. P. Salam and M. Spannowsky, *Phys. Rev. Lett.* **104**, 111801 (2010) [arXiv:0910.5472 [hep-ph]].
 27. D. E. Soper and M. Spannowsky, arXiv:1005.0417 [hep-ph].